Monthly Notices
of the
ROYAL ASTRONOMICAL SOCIETY

MNRAS **438,** 779–788 (2014)
Advance Access publication 2013 December 14

doi:10.1093/mnras/stt2246

What powers the most relativistic jets? – I. BL Lacs

Emma Gardner★ and Chris Done

Department of Physics, University of Durham, South Road, Durham DH1 3LE, UK

Accepted 2013 November 17. Received 2013 October 18; in original form 2013 August 20

ABSTRACT

The dramatic relativistic jets pointing directly at us in BL Lacertae (BL Lac) objects can be well modelled by bulk motion beaming of synchrotron self-Compton emission powered by a low Eddington fraction accretion flow. Nearly 500 of these active galactic nuclei (AGN) are seen in the second *Fermi* Large Area Telescope catalogue of AGN. We combine the jet models which describe individual spectra with the expected jet parameter scalings with mass and mass accretion rate to predict the expected number of *Fermi* detected sources given the number densities of AGN from cosmological simulations. We select only sources with Eddington scaled mass accretion rate <0.01 (i.e. radiatively inefficient flows), and include cooling, orientation effects and the effects of absorption from pair production on the extragalactic infrared background. These models overpredict the number of *Fermi* detected BL Lacs by a factor of 1000! This clearly shows that one of the underlying assumptions is incorrect, almost certainly that jets do not scale simply with mass and accretion rate. The most plausible additional parameter which can affect the region producing the *Fermi* emission is black hole spin. We can reproduce the observed numbers of BL Lacs if such relativistic jets are only produced by the highest spin ($a_* > 0.8$) black holes, in agreement with the longstanding spin–jet paradigm. This also requires that high spins are intrinsically rare, as predicted by the cosmological simulations for growing black hole mass via chaotic (randomly aligned) accretion episodes, where only the most massive black holes have high spin due to black hole–black hole mergers.

Key words: black hole physics – BL Lacertae objects: general – galaxies: jets – gamma-rays: galaxies.

1 INTRODUCTION

Relativistic jets are the most dramatic consequence of accretion on to stellar mass [black hole binaries (BHBs)] and supermassive black holes (SMBHs). Blazars are extreme examples of this, where the jet is viewed very close to the line of sight so its emission is maximally boosted by the relativistic bulk motion and can dominate the spectrum of the active galactic nucleus (AGN) from the lowest radio energies up to TeV. However, despite years of study, the fundamental issues of powering and launching the jets are not understood. There is general agreement only that it requires magnetic fields, but whether these can be generated solely from the accretion flow or whether the jets also tap the spin energy of the black hole (BH; Blandford & Znajek 1977) is still an open question. It is also difficult to test this observationally as neither BH spin nor total jet power is easy to measure, leading to divergent views e.g. in BHBs compare Russell, Gallo & Fender (2013) with Narayan & McClintock (2012), and in SMBHs compare Sikora, Stawarz & Lasota (2007) with Broderick & Fender (2011).

By contrast, the radiation emitted from the jet is fairly well understood, with spectra separating the Blazars into two types: BL Lacertaes (BL Lacs) and flat-spectrum radio quasars (FSRQs). BL Lacs are typically completely dominated by the jet emission, emitting a double humped synchrotron self-Compton (SSC) spectrum. The FSRQs are more complex, showing clear signatures of a 'normal' AGN disc and broad line region (BLR), unlike the BL Lacs which generally show no broad lines or disc emission. This lack of a standard disc/BLR in the BL Lacs is not just an effect from the relativistically boosted jet emission drowning out these components: the FSRQs have similarly boosted jet emission yet the disc and BLR are still clearly visible. Additionally, the presence of the disc and BLR in FSRQs means that there is an additional source of seed photons for cooling of relativistic particles in the jet, so their jet emission includes both SSC and external Compton (EC) components (Dermer, Schlickeiser & Mastichiadis 1992; Sikora, Begelman & Rees 1994), clearly contrasting with the SSC only jets in BL Lacs.

Thus the nature of the accretion flow itself is different in BL Lacs and FSRQs, with the latter showing a standard disc which is

★ E-mail: e.l.gardner@dur.ac.uk

absent from the former. This can be linked to the clear distinction in Eddington ratio between BL Lacs and FSRQs, with the BL Lacs all consistent with $\dot{m} = \dot{M}/\dot{M}_{\rm Edd} < 0.01$ (where $\eta \dot{M}_{\rm Edd} c^2 = L_{\rm Edd}$ and efficiency η depends on BH spin) while the FSRQs have $\dot{m} > 0.01$ (see e.g. Ghisellini et al. 2010, hereafter G10). This observed transition in accretion flow properties occurs very close to the maximum luminosity of the alternative (non-disc) solutions of the accretion flow equations. These result in a radiatively inefficient, hot, optically thin, geometrically thick flow (e.g. ADAFs, Narayan & Yi 1995) instead of a standard Shakura–Sunyaev, cool, optically thick, geometrically thin disc. Thus the BL Lacs have luminosity below this transition and can be associated with the radiatively inefficient flows, while FSRQs accrete at higher rates and have standard discs (see e.g. Ghisellini & Tavecchio 2008b; G10; Ghisellini et al. 2011; Best & Heckman 2012).

A similar transition is probably present in all types of AGN, not just the radio-loud objects. This predicts that a ultraviolet (UV) bright accretion disc is only present at $\dot{m} > 0.01$. Most (all?) radio-quiet Seyferts and quasars accrete above this limit (see e.g. Woo & Urry 2002). Strong UV is required to excite the broad emission lines, and the material which makes the BLR may also be a wind from the disc (e.g. Murray & Chiang 1997; Czerny & Hryniewicz 2012), so when the disc is replaced by a hot flow there is no strong UV emission and no broad lines – hence perhaps the class of AGN with low-ionization nuclear emission-line regions (LINERs) which are associated with $\dot{m} < 0.01$ (e.g. Satyapal et al. 2005). Additional evidence for this accretion flow transition comes from the much lower mass BHBs, which show a dramatic spectral switch around $\dot{m} \sim 0.01$ (Narayan & Yi 1995; Esin, McClintock & Narayan 1997, see e.g. Done, Gierliński & Kubota 2007, for a discussion of how this can explain the observed behaviour of BHBs).

Since all BL Lacs are associated with a low $\dot{m}$ accretion flow, we test here the hypothesis that all low $\dot{m}$ flows can launch a jet whose properties are determined simply by mass and mass accretion rate. We use the simplest possible scalings for how the jet (emission region size, magnetic field and injected power) scales with these parameters (Heinz & Sunyaev 2003; Heinz 2004), anchoring our scalings on to the fits to individual BL Lac objects of G10. We then can predict the jet spectra from BHs at any mass and mass accretion rate. We restrict our work to systems with $\dot{m} < 0.01$, i.e. BL Lac-type jets, to avoid the additional uncertainties of external seed photon density scaling with M and $\dot{m}$. We use cosmological simulations to predict the number densities of BHs with $\dot{m} < 0.01$, and assume that each of these will produce an appropriately scaled BL Lac-type jet. We include electron cooling, losses due to pair production on extragalactic background light and orientation effects from beaming to predict how many BL Lacs should be detected by *Fermi*. This is a statistical approach to constraining jet power in the population as a whole (cf. Martínez-Sansigre & Rawlings 2011), contrasting with most other previous approaches which determine jet power from detailed spectral fitting to individual sources.

We compare our predicted mass and redshift distributions with observations, and find we overpredict the observed number of BL Lacs by a factor of 1000. This strongly argues for another parameter apart from mass and mass accretion rate being required to produce BL Lac-type jets. The most plausible additional factor which can affect the small size scales of the *Fermi* emission region is BH spin. If this is indeed the answer – and there is longstanding speculation that high spin is required to produce the most relativistic jets – then this requires that high spin objects are rare. This is not the case if the SMBH grows in mass in prolonged accretion episodes, as the accreted angular momentum can quickly spin the BH up to maximal (Volonteri et al. 2005; Volonteri, Sikora & Lasota 2007; Fanidakis et al. 2011; Volonteri 2012). Instead, it requires that the SMBH mass build up via accretion is from multiple, randomly aligned smaller episodes, resulting in low spin (King, Pringle & Hofmann 2008). The only high spin BHs in these simulations are the most massive, where the last increase in mass was via a BH–BH coalescence following a major host galaxy merger (Volonteri et al. 2005, 2007; Fanidakis et al. 2011, 2012; Volonteri 2012).

2 SYNCHROTRON SELF-COMPTON JETS

We adopt a single zone SSC model of the type used by Ghisellini & Tavecchio (2009), which self-consistently determines the electron distribution from cooling. We briefly summarize our model here, with full details in Appendix A.

We assume a spherical emission region of radius R. We neglect the contribution from regions further out along the jet, as these only make a difference to the low energy (predominantly radio) emission. We assume material in the jet moves at a constant bulk Lorentz factor (Γ), and that a fraction of the resulting jet power is used to accelerate electrons in the emission region. The power injected into relativistic electrons is then $P_{\rm rel} = 4/3\pi R^3 \int \gamma m_{\rm e} c^2 Q(\gamma)\,{\rm d}\gamma$, where the accelerated electron distribution is a broken power law of the form

$$Q(\gamma) = Q_0 \left(\frac{\gamma}{\gamma_{\rm b}}\right)^{-n_1} (1+\gamma/\gamma_{\rm b})^{n1-n2} \text{ for } \gamma_{\rm min} < \gamma < \gamma_{\rm max}. \quad (1)$$

These electrons cool by emitting self-absorbed synchrotron and SSC radiation, so the seed photon energy density $U_{\rm seed} = U_B + g(\gamma) U_{\rm sync}$ includes both the magnetic energy density $U_B = B^2/8\pi$, and the fraction $g(\gamma)$ of the energy density of synchrotron seed photons, $U_{\rm sync}$, which can be Compton scattered by electrons of energy γ within the Klein–Nishina limit. This gives rise to a steady state electron distribution, $N(\gamma) = -\dot{\gamma}^{-1} \int_{\gamma}^{\gamma_{\rm max}} Q(\gamma')\,{\rm d}\gamma'$, where the rate at which an electron loses energy $\dot{\gamma} m_{\rm e} c^2 = 4/3 \gamma^2 \sigma_{\rm T} c U_{\rm seed}$. However, this assumes that the electrons can cool within a light crossing time, but the cooling timescale $t_{\rm cool} = \gamma/\dot{\gamma}$ itself depends on γ, with high-energy electrons cooling fastest. We calculate the Lorentz factor that can just cool in a light crossing time of the region, $\gamma_{\rm cool}$, and join smoothly on to the accelerated electron distribution below this. The full self-consistent electron distribution can be characterized by $N(\gamma) = K\,n(\gamma)$, where K is the number density of electrons at $\gamma = 1$ and $n(\gamma)$ incorporates all the spectral shape. We calculate the resulting (self-absorbed) synchrotron and self-Compton emission using the delta function approximation as this is much faster than using the full kernel but is accurate enough for our statistical analysis (Dermer & Mernon 2009).

This jet frame emission is boosted by the bulk motion of the jet, with the amount of boosting depending on both Γ and the orientation of the jet. The emission is then cosmologically redshifted and attenuated due to pair production on the extragalactic infrared background light (though this is generally small for the *Fermi* bandpass) to produce the observed flux.

The parameters of our model are therefore the following.

(i) Physical parameters of the jet: Γ and radius of emission region R.

(ii) The magnetic field of the emission region and power injected into relativistic electrons (B and $P_{\rm rel}$).

(iii) Parameters of the injected electron distribution: $\gamma_{\rm min}$, $\gamma_{\rm b}$, $\gamma_{\rm max}$, n_1 and n_2.

We adopt the cosmology used in the Millennium Simulations: $h = 0.72$, $\Omega_{\rm m} = 0.25$, $\Omega_{\rm vac} = 0.75$ (Springel et al. 2005; Fanidakis et al. 2011).

3 SCALING JETS

We assume that the acceleration mechanism is the same for all BL Lacs, giving the same injected electron distribution, regardless of mass and accretion rate. We also assume all jets are produced with the same Γ. This leaves three remaining parameters: R, B and $P_{\rm rel}$.

We scale $R \propto M$, since all size scales should scale with the mass of the BH (Heinz & Sunyaev 2003). We assume the jet power is a constant fraction of the total accretion power, $P_{\rm j} \propto \dot{m}M$. This assumption is valid whether the jet is powered by the accretion flow or the spin energy of the BH, since extraction of BH spin energy relies on magnetic fields generated in the accretion flow, which will be affected by accretion rate. A constant fraction of the total jet power is then injected into relativistic particles and magnetic fields. Hence $P_{\rm rel} \propto P_{\rm j} \propto \dot{m}M$.

Energy density in the jet frame is related to power in the rest frame via $P = \pi R^2 \Gamma c U$, so $P_B \propto R^2 U_B \propto \dot{m}M$, hence $B \propto U_B^{1/2} \propto (\dot{m}/M)^{1/2}$. Therefore all energy densities should scale as $U_B \propto U_{\rm rel} \propto (\dot{m}/M)^{1/2}$.

We anchor this with parameters from the fit to the classic LBL object, 1749+096 from G10, which is relatively near to the top of the BL Lac accretion rate range. This gives $M_0 = 7 \times 10^8$, $R_0 = 172 \times 10^{15}$ cm, $B_0 = 1$ G, $P_{\rm rel,\,0} = 3.5 \times 10^{42}$ erg s^{-1}, $\Gamma = 15$, $\gamma_{\rm min} = 1$, $\gamma_{\rm b} = 2 \times 10^3$, $\gamma_{\rm max} = 1 \times 10^5$, $n_1 = 0.9$, $n_2 = 2.8$, and we scale R, $P_{\rm rel}$ and B as

$$R = R_0 \frac{M}{M_0}, \tag{2}$$

$$P_{\rm rel} = P_{\rm rel,0} \frac{\dot{m}}{\dot{m}_0} \frac{M}{M_0}, \tag{3}$$

$$B = B_0 \left(\frac{\dot{m}}{\dot{m}_0} \frac{M_0}{M} \right)^{1/2}. \tag{4}$$

We calculate the accretion rate of 1749+096 following the method of G10. Assuming the jet is maximal ($P_{\rm j} = \dot{M}c^2$), we sum the power in magnetic fields, relativistic electrons and the bulk motion of cold protons to calculate $P_{\rm j}$, giving

$$\dot{m}_0 = \frac{P_{\rm j}\eta}{1.38 \times 10^{38}\,(M/{\rm M}_\odot)} \sim 3.5 \times 10^{-3}, \tag{5}$$

for their value of $\eta = 0.08$. Fig. 1 shows our model spectrum, together with the model and data from G10. The two models differ slightly due to our use of the delta function approximation to speed up calculation time. Nevertheless the two models are in agreement within ~0.3 dex, and crucially our model reproduces the correct level of *Fermi* flux (red bow tie).

4 TRANSITION FROM HIGH FREQUENCY PEAKED TO LOW FREQUENCY PEAKED BL LACS WITH ACCRETION RATE

We limit our model to a maximum accretion rate of $\dot{m} = 10^{-2}$, since above this the accretion flow is expected to make a transition to a radiatively efficient thin disc. The strong UV and consequent BLR emission provide additional seed photons, switching the main *Fermi* radiation process from SSC (BL Lacs) to EC (FSRQs).

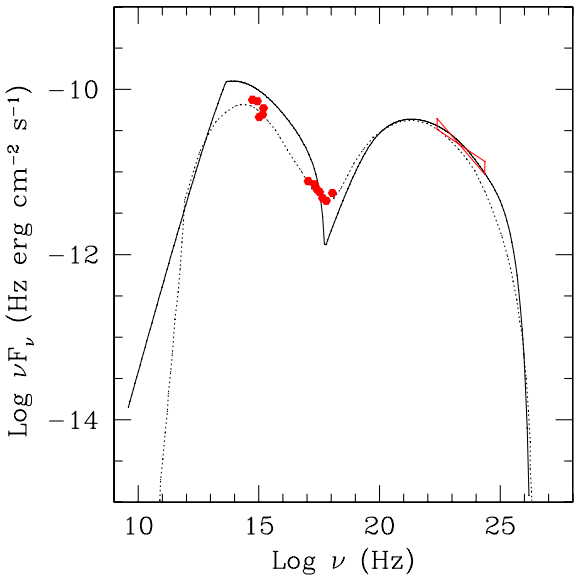

Figure 1. Model spectrum using parameters for 1749+096 ($z = 0.322$) from Ghisellini et al. (2010) (solid black line). Dotted line shows their spectrum for the same parameters and red points show their data.

Fig. 2(a) shows a sequence of spectra with R, $P_{\rm rel}$ and B scaling as described above for $\dot{m} = 10^{-2}$ (black)–10^{-4} (magenta) for constant mass. This shows the systematic decrease in luminosity, coupled to a change in spectral shape from a low synchrotron peak energy [optical: low frequency peaked BL Lac (LBL)] to a high synchrotron peak energy [X-ray: high frequency peaked BL Lac (HBL)] as shown by Ghisellini & Tavecchio (2008b, 2009).

We can compare the *Fermi* flux levels of our lower accretion rate spectra with observed HBLs. The HBL 1959+650 (see Tavecchio et al. 2010 for a spectrum, G10 for spectral fitting parameters) has a mass of $2 \times 10^8\,{\rm M}_\odot$, so only slightly larger than the $10^8\,{\rm M}_\odot$ system shown in Fig. 2(a). 1959+650 has an injected $P_{\rm rel}$ of 7×10^{40} erg s^{-1} (G10), corresponding in our scalings to $\dot{m} = 2.45 \times 10^{-4}$. So it should have a similar *Fermi* flux to the red spectrum of Fig. 2(a), which corresponds to $\dot{m} = 3 \times 10^{-4}$, $M = 10^8$. The observed $\log(\nu L(\nu))$ *Fermi* flux of 1959+650 at 10^{23} Hz is 43.5 Hz erg s^{-1}, which is consistent with our red spectrum.

The changing shape of the emitted spectrum with accretion rate is due to the decrease in seed photons for electron cooling at lower $\dot{m}$, as shown explicitly by the corresponding self-consistent electron distributions in Fig. 2(b). The Lorentz factor of electrons which can cool in a light crossing time is $\gamma_{\rm cool} \propto 1/(R\,U_{\rm seed}) \propto (1/M)(M/\dot{m}) \propto 1/\dot{m}$. The lowest mass accretion rate ($\dot{m} = 10^{-4}$, magenta) shows cooling only for the highest Lorentz factors, with $\gamma_{\rm cool} \sim 10^{4.5}$. Below this the shape of the electron distribution is the same as the injected distribution, with a smooth break at $\gamma_{\rm b} \sim 10^3$. As $\dot{m}$ increases, the sharp break at $\gamma_{\rm cool}$ moves to lower Lorentz factors. For the black electron distribution corresponding to $\dot{m} = 10^{-2}$, $\gamma_{\rm cool}$ is comparable to $\gamma_{\rm b}$. This is clear from the black spectrum in Fig. 2(a), where the spectral peak is now produced by the cooled electron distribution above $\gamma_{\rm cool}$.

Increasing cooling, as a result of increasing accretion rate, therefore provides a natural explanation for the existence of HBLs and LBLs (Ghisellini & Tavecchio 2008b, 2009). In the context of our model, HBLs correspond to BHs with very low accretion rates. There is very little cooling and the bulk of the

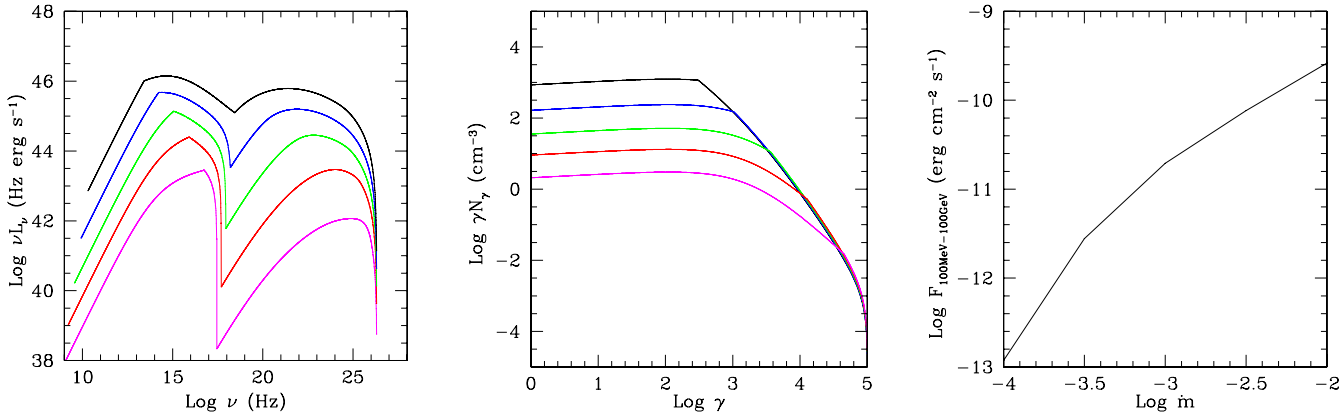

Figure 2. (a) BL Lac model SEDs for fixed BH mass and increasing accretion rate ($\dot{m} = 10^{-4}$ (magenta), 3×10^{-4} (red), 10^{-3} (green), 3×10^{-3} (blue) and 10^{-2} (black), $M_{\rm BH} = 10^8\,{\rm M}_\odot$). (b) Corresponding steady state electron distributions. (c) *Fermi* flux as a function of accretion rate, using mass and distance of model spectrum.

synchrotron emission is produced by electrons with Lorentz factors close to $\gamma_{\rm max}$. Their electron distributions most closely resemble the original injected distributions. LBLs correspond to BHs with higher accretion rates, where cooling becomes increasingly important and the bulk of the energy is produced by electrons close to $\gamma_{\rm cool}$.

Since HBLs are at lower accretion rates they are intrinsically fainter and so should be observed at lower redshifts than LBLs. This is indeed observed (Shaw et al. 2013). *Fermi* sensitivity is also a strong function of spectral index, decreasing with spectral hardness (Nolan et al. 2012). Since LBLs have softer spectra this suggests *Fermi* will preferentially select LBLs over HBLs due to spectral shape as well as flux.

Fig. 2(a) also shows that as $\dot{m}$ increases, the ratio of the Compton to synchrotron luminosities changes. With our scalings, $L_{\rm sync} \propto R^3 U_B K$ and $L_{\rm comp} \propto R^3 U_{\rm sync} K \propto R^3 (R U_B K) K$, i.e. $L_{\rm sync}/L_{\rm comp} \propto 1/(RK)$, where K is the normalization of the steady state electron distribution. If there is complete cooling, i.e. $\gamma_{\rm cool} < \gamma_{\rm min}$, then $K \propto Q_0/U_{\rm seed} \propto (\dot{m}/M^2)(\dot{m}/M)^{-1} \propto 1/M$ which is independent of accretion rate. However, the BL Lac spectra do not show complete cooling (see Fig. 2b). If there is no cooling, $K \sim R Q_0/c \propto \dot{m}/M$. The BL Lac spectra lie in this regime where the cooling is incomplete, hence $L_{\rm sync}/L_{\rm comp} \propto 1/\dot{m}$. This can be seen in Fig. 2(b), where the normalization of the electron distribution at $\gamma = 1$ increases with $\dot{m}$. The scaling is not exactly $K \propto \dot{m}$, since there is an additional dependence on $\dot{m}$ introduced by $\gamma_{\rm cool}$ decreasing through the intermediate regime.

Fig. 2(c) shows how the flux in the *Fermi* band drops with accretion rate. For higher accretion rates, cooling is efficient, so $L_{\rm comp} \propto \dot{m}$. For low accretion rates, cooling is inefficient so $L_{\rm comp} \propto \dot{m}^3$.

However, a more detailed comparison of Fig. 2(a) to the data in the 'blazar sequence' shows evidence that the Compton flux changes more slowly with decreasing mass accretion rate due to an increase in the maximum Lorentz factor of the accelerated electron distribution (Ghisellini & Tavecchio 2008b, 2009). Again, this can be a consequence of the different cooling environment, where electrons are accelerated to a maximum energy which is set by a balance between the acceleration time-scale and the cooling time-scale. Thus the accelerated electron distribution may itself change with cooling, such that $\gamma_{\rm b} \propto \gamma_{\rm max} \propto 1/U_{\rm seed}$. We will consider such models later in the paper.

5 BL LAC VISIBILITY

The visibility of a BL Lac is strongly affected by viewing angle. Fig. 3(a) shows how sharply the observed luminosity decreases for our assumed $\Gamma = 15$ with increasing viewing angle, where θ is measured in radians from the jet axis. Thus there is a difference of 10^{12} between the observed flux from a face on jet compared to an edge on jet.

The more distant the source, the more closely aligned to our line of sight the jet must be in order to boost the observed flux to a visible level. We define a flux limit of $F_{100\,{\rm MeV}-100\,{\rm GeV}} > 5 \times 10^{-12}\,{\rm erg\,s^{-1}\,cm^{-2}}$ from the *Fermi* 2-year catalogue (Nolan et al. 2012), and show in Fig. 3(b) the limiting redshift, $z_{\rm limit}$, at which a BL Lac at $\dot{m} = 10^{-2}$ with different masses can be detected by *Fermi* at different inclination angles. We include the effects of absorption from pair production on the extragalactic infrared (IR) background using the model of Kneiske & Dole (2010), though this is negligible. Only the most massive BHs, $\sim 10^{10}\,{\rm M}_\odot$ which are most closely aligned to our line of sight can be seen out beyond $z = 4$. $z_{\rm limit}$ drops by a factor of $\sim$3 if the inclination angle is increased from 0 to the more statistically likely $1/\Gamma$. This represents a change of just $\sim 4^\circ$ for $\Gamma = 15$ used in our calculations. For a typical BL Lac mass of $10^9\,{\rm M}_\odot$ viewed at $1/\Gamma$ the maximum observable redshift is $z \sim 1$, increasing to 4 only for the most face on jets.

Fig. 3(c) shows how the redshift limit drops as a function of accretion rate for each mass [10^{10} (black), 10^9 (blue), 10^8 (magenta) and $10^7\,{\rm M}_\odot$ (red)] BH for $\theta = 0$. If LBLs correspond to BL Lacs at $\dot{m} \sim 10^{-2}$ and HBLs at $\dot{m} < 10^{-3}$ this shows how the redshift limits for the two populations should differ, with the majority of HBLs being observed below $z = 3$. Shaw et al. (2013) find this to be the case, with the distribution of LBLs extending to higher z, although they find the means of both populations are well below $z = 3$.

6 PREDICTED BL LAC POPULATION FROM COSMOLOGICAL SIMULATIONS

Cosmological simulations predict the number of SMBHs accreting at different redshifts, together with their masses and accretion rates. These simulations have been found to agree well with the observed number densities of broad line and narrow line AGN in the local Universe (Fanidakis et al. 2011, 2012). Combining our spectral code

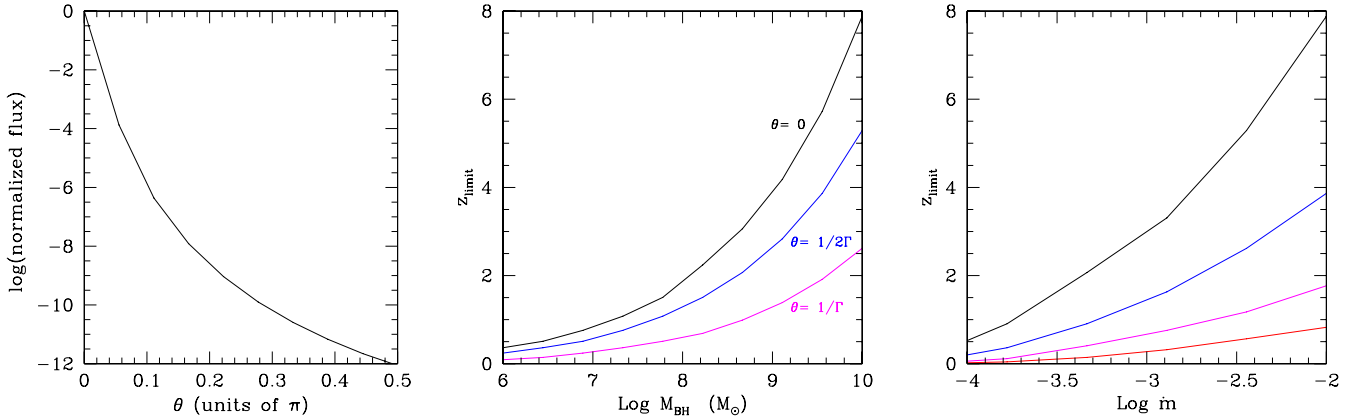

Figure 3. (a) Decrease in observed flux with increasing viewing angle, where θ is measured in radians from the jet axis, for $\Gamma = 15$. (b) Redshift limits for *Fermi* visible BL Lacs as a function of BH mass, for increasing viewing angle and $\dot{m} = 10^{-2}$. (c) Redshift limits for *Fermi* visible BL Lacs as a function of accretion rate, for $M_{\rm BH} = 10^7$ (red), 10^8 (magenta), 10^9 (blue) and $10^{10}\,{\rm M}_\odot$ (black) and $\theta = 0$.

with the BH data from these simulations allows us to predict the number of AGN that should be detected as BL Lacs by *Fermi*.

We combine our code with the BH number densities predicted by the Millennium Simulation (Springel et al. 2005; Fanidakis et al. 2011, 2012), binned as a function of both mass and mass accretion rate. We define a luminosity density from the number density multiplied by the luminosity at that mass and mass accretion rate, i.e. $L = \eta \dot{M} c^2$ for the thin disc regime $10^{-2} < \dot{m} < 1$, joining smoothly on to a radiatively inefficient regime at lower $\dot{m}$ where $L \propto \dot{m}^2$ (Narayan & Yi 1995) and on to a super-Eddington flow at higher $\dot{m}$ where $L \propto \ln(1 + \dot{m})$ (Shakura & Sunyaev 1973). The luminosity density in each $(z, M, \dot{m})$ bin therefore depends on the mass, accretion rate, spin (which sets η), the inferred accretion regime and the number of BHs in that bin.

Fig. 4 shows the evolution of the luminosity density of accretion power across cosmic time showing the features described by Fanidakis et al. (2011, 2012). At high redshift there is plenty of gas to fuel accretion. The BHs accrete close to the Eddington limit and grow rapidly. Comparing the snapshots for $z \sim 9$ and $\sim$5, the typical BH mass producing the bulk of the accretion luminosity increases from $\sim 10^6$ to $\sim 10^8\,{\rm M}_\odot$. As the BHs gradually run out of gas, their accretion rates drop (compare $z \sim 2$ and $\sim$1). By redshift 2, accretion rates are beginning to drop below $\dot{m} = 10^{-2}$, into the regime at which BL Lac-type jets should be produced. This suggests no BL Lacs should be observed much above $z \sim 2$, not just because the flux becomes too faint, but because the typical accretion rate is too high for the production of BL Lac jets.

We select only BHs in the radiatively inefficient regime ($\dot{m} < 10^{-2}$), assuming all BHs accreting inefficiently will produce a BL Lac-type jet, and calculate the number of AGN hosting a BL Lac-type jet in each $(z, M, \dot{m})$ bin. If this number is less than 1 we use Poisson statistics to randomly determine whether a BH is present or not. Each BH in each $(z, M, \dot{m})$ bin is then assigned a random distance within this redshift bin and random $\theta_{\rm obs}$, assuming $\cos\theta_{\rm obs}$ is distributed uniformly. We then calculate the observed spectrum to determine whether or not the jet would be visible to *Fermi*.

Fig. 5(a) shows the predicted redshift distribution of *Fermi* visible BL Lacs (black). The predicted distribution peaks at $z \sim 0.5$ and drops gradually to $z \sim 2$. No BL Lacs are observed above this point, not because they are not visible (see Fig. 3b), but because there simply are not enough SMBHs accreting below 10^{-2} in the cosmological simulations to produce SSC jets, due to the higher activity expected at earlier times. The low redshift distribution of BL Lacs is a direct result of cosmic downsizing and the requirement of an $\dot{m} < 10^{-2}$ to produce a SSC jet.

However, comparing this to observations shows a huge discrepancy (red solid line from Shaw et al. 2013, which almost merges with the *X*-axis at this scale). Our expected number of $\sim$100 000 BL Lacs dramatically overpredicts the observed number of *Fermi* detections ($\sim$500). A clear illustration of the problem can be seen from simply the number density of massive ($8 < \log M < 9$) BH accretion flows with $10^{-3} < \dot{M} < 10^{-2}$ in the cosmological simulations in the redshift bin centred around $z \sim 0.5$ (Fanidakis et al. 2011). This number is $6.8 \times 10^{-4}\,{\rm Mpc}^{-3}$ and the volume of this bin, from $0.509 < z < 0.564$, is $\sim$9 Gpc^3 so this gives 6101 659 objects which should host similar jets to 1749+096 (Fig. 1), i.e. have *Fermi* flux of $10^{-10.5}(0.5/0.322)^{-2} \sim 10^{-11}$ erg cm^{-2} s^{-1} if viewed at the same angle (roughly $1/\Gamma$). The probability that we see the source within this angle is $1 - \cos(1/\Gamma)$, so the expected number of *Fermi* detections of these sources alone is $\approx$13 554, similar to the full calculation results. The large discrepancy clearly points to a fundamental breakdown of one of the assumptions.

On a more subtle level, the shape of the redshift distribution for the *Fermi* predictions is also mismatched to the observations. The red dashed line shows the observed number of BL Lacs scaled by a factor of 100 so it can be compared to the predicted distribution. We define redshift from Shaw et al. (2013) as either spectroscopic redshift, spectroscopic lower limit, the mean of their redshifts derived from host galaxy fitting or their redshift upper limits, in that order of preference. The dashed line shows this observed redshift distribution ($\times$100). It is clear that not only is the total predicted number wrong, but we are also overestimating the proportion of BL Lacs in the range $z = 0.5$–2.

The mass distribution and mass accretion rate distributions are as expected (Figs 5b and c), with higher luminosity SSC flows (i.e. higher $\dot{m}M$) being more likely to be observed, so simple energetics selects the highest mass and mass accretion rate objects, so the typical predicted mass of a *Fermi* visible BL Lac $\sim 10^{8.5}$–$10^9\,{\rm M}_\odot$ is a combination of three factors.

(i) Very few BHs accreting at $\dot{m} < 10^{-2}$ above $z = 2$.
(ii) Most BHs at $z < 2$ accreting with $\dot{m} < 10^{-2}$ have $M > 10^8$.
(iii) BHs with $M > 10^9$ are increasingly rare in the local Universe so we are less likely to observe one favourably orientated to our line of sight.

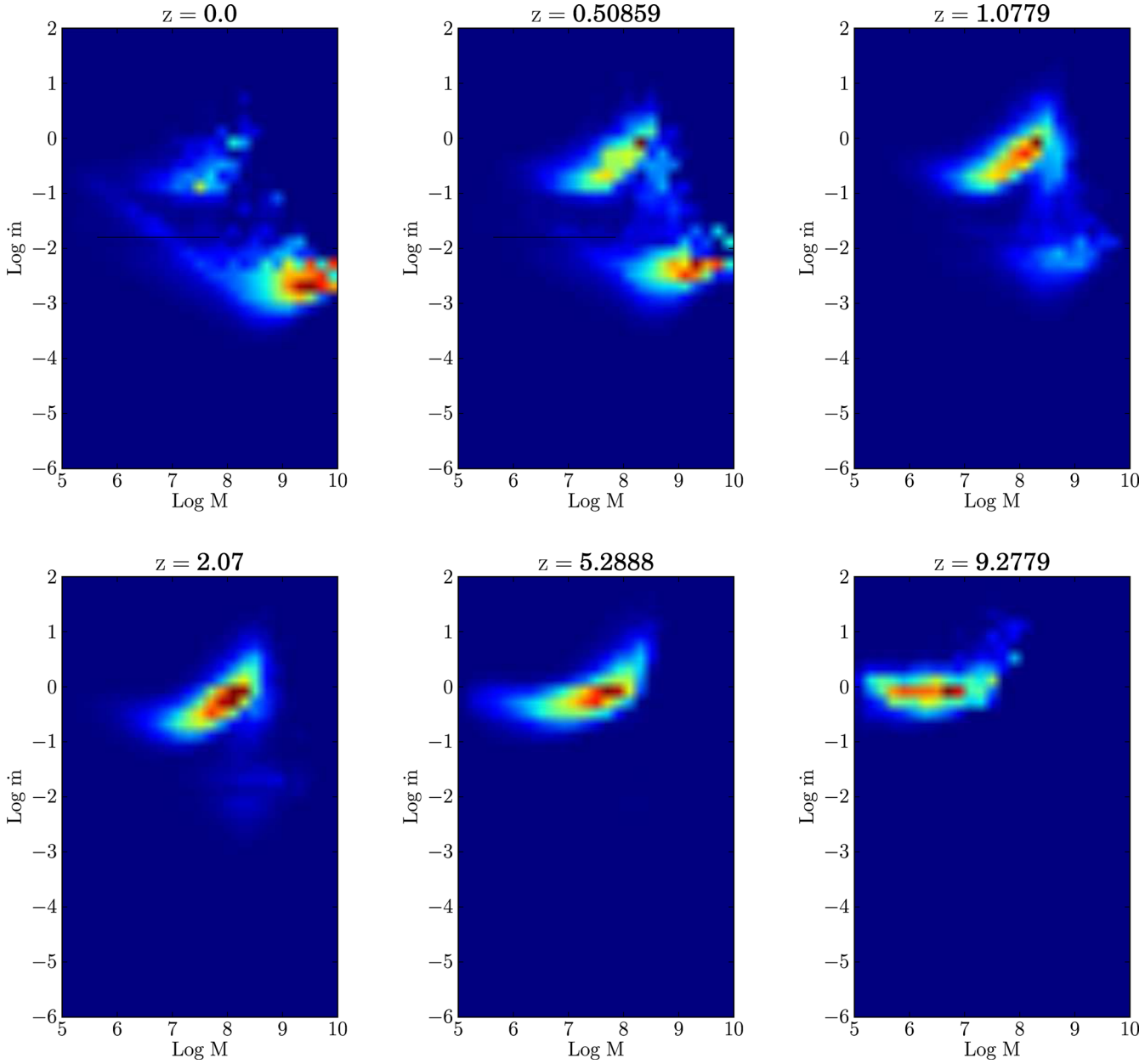

Figure 4. Predicted mass and accretion rate distribution of accreting BHs at increasing redshift from Millennium Simulation. Colours trace luminosity density, with red showing the mass and accretion rates at which the maximum accretion luminosity is emitted at each redshift.

7 ANOTHER FACTOR AFFECTING JET SCALING?

Our results predict $\sim 10^5$ BL Lacs should have been detected in the *Fermi* 2-year catalogue. In contrast, ∼500 objects in the second *Fermi* Large Area Telescope (LAT) catalogue are classed as BL Lacs. Even allowing for galactic centre emission limiting sky coverage ($|b| > 10^\circ$ means that only 80 per cent of the sky is included), this is still three orders of magnitude larger than observed. Clearly jets do not simply scale with accretion power.

We assumed the injected electron distribution was independent of mass accretion rate. This may not be the case. Ghisellini & Tavecchio (2009) approximately use $\gamma_{\rm max} \propto \gamma_{\rm b} \propto 1/\dot{m}$ to fit their blazar sequence. Acceleration of electrons is affected by the ambient photon field which depends on the amount of cooling and ultimately on accretion rate. In the efficient cooling regime, $L_{\rm sync} \propto L_{\rm comp} \propto \dot{m}M$, making $\gamma_{\rm max} \propto 1/\dot{m}$ not unreasonable. However, an increase of $\gamma_{\rm max}$, and $\gamma_{\rm b}$ in particular, only serves to increase the *Fermi*-band luminosity for lower $\dot{m}$ systems, and increase the discrepancy between the predictions and observations.

The discrepancy could instead be explained if every BH accreting below 10^{-2} has the potential to produce a BL Lac-type jet, but only does so 1/1000th of the time. This seems unlikely, since Fanaroff–Riley Type I (FRI) AGN, the misaligned versions of BL Lacs (Padovani & Urry 1990, 1991; Urry, Padovani & Stickel 1991) show large-scale extended radio jets. This suggests these jets are persistent, analogous to the steady low/hard state jet seen in BHBs at low $\dot{m}$, not transient events.

Another possibility is that the jet depends on magnetic flux being advected on to the BH from the extremely large-scale hot halo gas around the galaxy. Sikora & Begelman (2013) suggest that if there is magnetic flux in this gas, then it could be dragged down close

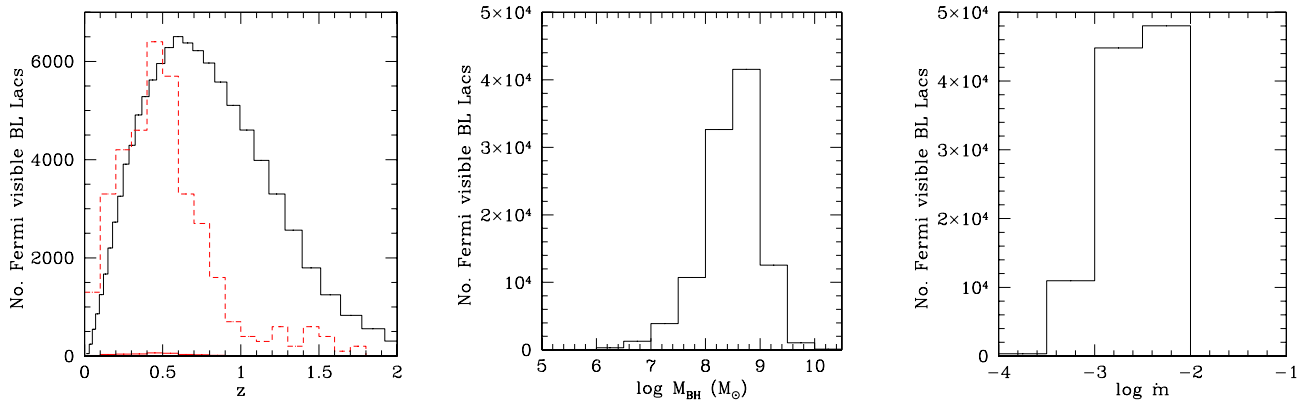

Figure 5. (a) Predicted redshift distribution of *Fermi* visible BL Lacs, assuming BHs of all spins accreting below $\dot{m} = 10^{-2}$ produce a BL Lac-type jet (black). Red solid line shows observed redshift distribution of *Fermi* detected BL Lacs. Red dashed line shows observed redshift distribution × 100. (b) Predicted mass distribution of *Fermi* visible BL Lacs. (c) Predicted accretion rate distribution of *Fermi* visible BL Lacs.

to the BH by cold gas from a merging spiral galaxy. However, this does not address the fundamental question as to where the magnetic flux in the halo gas comes from, and using cold gas from a spiral merger to drag this field down to the BH is unlikely to be applicable in the BL Lacs as they have low ongoing mass accretion rates.

The bulk Lorentz factor of the jet is the biggest factor affecting its visibility. We rerun our calculations with a reduced $\Gamma = 10$ instead of 15 and find this roughly halves the predicted number of BL Lacs, but still wildly overpredicts the observations.

We have assumed all jets are produced with the same value of bulk Lorentz factor but this is clearly not the case – BHBs at low $\dot{m}$ have $\Gamma \sim 1.2$ (Fender, Belloni & Gallo 2004). The most obvious way to reduce the number of visible BL Lacs is to allow a distribution of Γ. Yet there must be some physical parameter which controls the jet acceleration. The acceleration region, where the magnetic (Poynting) flux of the jet is converted to kinetic energy, is very close to the BH, so it seems most likely that this is set by the BH itself, in which case BH spin is the only remaining plausible parameter. A potential explanation for the lower number of observed BL Lacs is that if only BHs with the highest spin produce highly relativistic jets, and high spin is rare.

The cosmological simulations include the growth of SMBH spin via accretion processes and BH–BH coalescence following galaxy mergers (Volonteri et al. 2005, 2007; Fanidakis et al. 2011, 2012; Volonteri 2012). The mass accumulated on to the central SMBH in an accretion event is tied in the simulation to a fixed fraction (0.5 per cent) of the mass of gas in a star formation episode in the host galaxy. If this mass is all accreted in a single event (prolonged accretion), then this is sufficient to spin most BHs up to maximal (Volonteri et al. 2005, 2007). However, the mass accreting on to the central BH in any single event may be limited by self-gravity. This splits the accreting material up into multiple smaller events, each of which can be randomly aligned since the star formation scale height is large compared to the BH sphere of influence even in a disc galaxy (King et al. 2008). Such chaotic accretion flow models result in predominantly low spin BHs (Volonteri et al. 2007; King et al. 2008; Fanidakis et al. 2011, 2012), and high spins are rare as they are produced not via accretion but via BH mergers (Fanidakis et al. 2011, 2012).

We use the spin distribution from the chaotic accretion flow model simulations, and introduce a spin cut to our results, so that only BHs with spin greater than $a_{\rm cut} \sim 0.8$ produce a BL Lac-type jet. This reduces the predicted number of *Fermi* visible BL Lacs to ∼900. Fig. 6(a) shows the resulting redshift distribution together with the observed distribution. Not only does this reduce the discrepancy between predicted and observed total numbers, it also gives a better match to the shape of the distribution. Limiting production of BL Lac-type jets to BHs with high spin causes the redshift distribution to peak slightly later and drop off more sharply above $z = 0.5$. This is because high spins arise from BH mergers. Production of BL Lac jets is already limited to BHs accreting below 10^{-2}, i.e. $M > 10^8$. The BH mergers which make the most massive BHs occur at the latest times.

Figs 6(b) and (c) show how this affects the predicted mass and accretion rate distributions of *Fermi* visible BL Lacs. The scaled down distributions including BHs of all spins are shown by the dashed lines for comparison. Requiring high spin increases the peak of the mass distribution to $\sim 10^{8.5}$–$10^{9.5}$, because it is the most massive BHs that are former by mergers and are consequently more likely to have high spin. The peak of the accretion rate distribution is actually slightly reduced. This is because the more massive BHs have lower accretion rates; the spin cut has excluded lower mass BHs with lower spins which tend to have slightly higher accretion rates.

The low spin, low accretion rate BHs, which generally have smaller masses (10^7–10^8 $M_\odot$) correspond to the LINERs, which are not observed to have jets as relativistic as those in BL Lacs. If they are low spin, as expected, and high spin is required for a highly relativistic jet, then this naturally explains why LINERs are observed to have weaker radio jets.

8 IMPLICATIONS OF SCALING JET POWER WITH SPIN: FRI SOURCES

The parent population of BL Lacs is probably the FRI sources (e.g. the review by Urry & Padovani 1995). These show 'fluffy' radio jets whose surface brightness decreases with distance from the central source, contrasting with the classic lobe and hotspot radio emission seen in the more powerful FRII sources which are the parent population of the FSRQ (Padovani & Urry 1992). Thus the FRI sources should also correspond to high spin BHs, and indeed are similarly powered by high mass SMBHs (Woo & Urry 2002).

However, we might then expect some difference in jet radio emission between the FRIs and lower mass LINERs as the cosmological simulations predict that the lower mass SMBHs have lower spin (Fanidakis et al. 2011, 2012). Sikora et al. (2007) claim that this

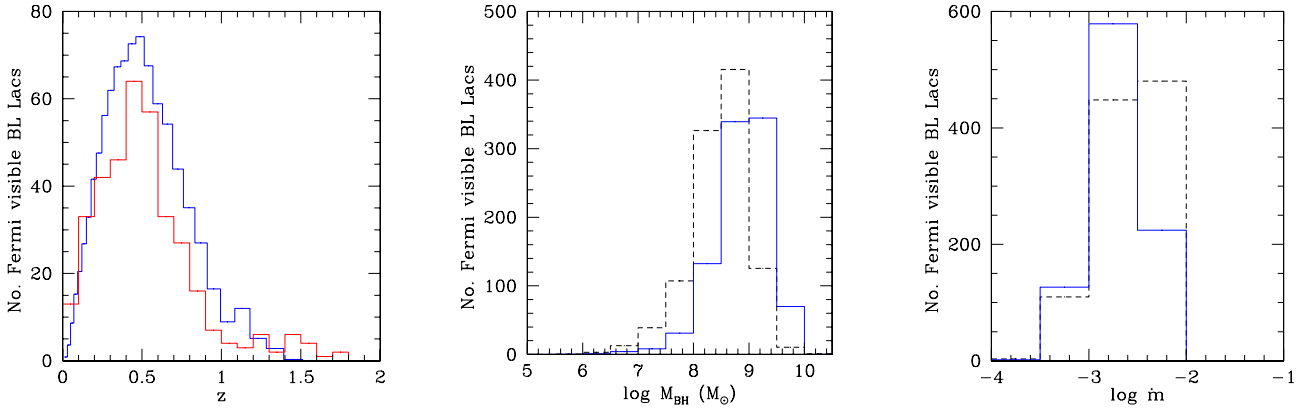

Figure 6. (a) Predicted redshift distribution of *Fermi* visible BL Lacs, assuming only BHs with spins $a > 0.8$ produce a BL Lac-type jet (blue). Red solid line shows observed redshift distribution of *Fermi* detected BL Lacs. (b) Predicted mass distribution including only BHs with $a > 0.8$ (blue). Black dashed line shows predicted distribution including all BHs $\times$ 0.01. (c) Predicted accretion rate distribution including only BHs with $a > 0.8$ (blue). Black dashed line shows predicted distribution including all BHs $\times$ 0.01.

difference is indeed seen, with radio emission being ∼3 orders of magnitude higher in the FRIs.

However, some of this difference disappears when only core radio luminosity (rather than core plus lobes) is used (Broderick & Fender 2011). This is clearly an issue as the extended radio emission must depend on environment. The BHs in FRIs are more massive than those in LINERs, hence live in richer cluster environments, with larger dark matter haloes which trap more hot cluster gas. The jet then emerges into a denser, higher pressure environment, which means that a much larger fraction (potentially all) of the jet kinetic energy is converted to radiation and/or heating of the cluster gas (Bîrzan et al. 2004). Conversely, any jet from the lower mass LINERs emerges into a poorer group environment, so adiabatic losses can predominate and the extended radio emission is much smaller (e.g. Krause et al. 2012).

Some of the remaining difference in core radio power is *expected* due to the difference in mass (Broderick & Fender 2011). However, even accounting for this there is still a factor of ∼10 in mass-corrected, core radio emission. The LINERs lie on the Fundamental Plane (Merloni, Heinz & di Matteo 2003; Falcke, Körding & Markoff 2004), i.e. have the expected core radio emission for their BH mass and mass accretion rate, so the FRIs are a factor of 10 brighter in mass-corrected, core radio emission than expected from the same jet models which produce the low bulk Lorentz factor BHB and LINER jets, consistent with the idea that the jet is intrinsically more powerful/has higher Lorentz factor due to BH spin.

It is difficult to predict the difference in core radio emission with BH spin in our models as synchrotron self-absorption means that the observed radio emission does not arise in the same region as produces the *Fermi* flux. It may be produced either at larger radii, perhaps where the jet has decelerated, or in a lower density, lower bulk Lorentz factor layer surrounding the $\Gamma = 15$ spine of the jet. Either of these could explain the lower Lorentz factor ($\Gamma \sim 2$–10) of the radio jet observed in FRIs (Chiaberge et al. 2000), though the spine-layer structure may additionally be able to explain the very fast variability time-scales seen in some BL Lacs (Ghisellini & Tavecchio 2008a).

9 CONCLUSIONS

We have taken a statistical approach to constrain the conditions necessary to produce the highly relativistic jets seen in BL Lac objects. We combine SMBH number densities from cosmological simulations, known to reproduce the optical luminosity function of AGN, with spectral models of jet emission and simple jet scaling functions which depend only on mass and accretion rate. The key assumption is that every BH accreting with $\dot{m} < 10^{-2}$, i.e. in the radiatively inefficient accretion flow regime, should produce a BL Lac-type jet.

Our calculation of the expected number of BL Lacs detectable by *Fermi* overpredicts the observations by three orders of magnitude. This clearly shows that our fundamental assumptions are incorrect, and that the jet power and properties do not scale simply with mass and mass accretion rate. The only other parameter which a BH can have is spin. We can reproduce the observed numbers of BL Lacs if SMBHs grow predominantly via chaotic (randomly aligned) accretion episodes, and that BL Lac-type jets are restricted to BHs with spin $a > 0.8$. These are rare as they form from BH–BH coalescence following a major merger event which is not then overwhelmed by further chaotic accretion, i.e. this requires a gas-poor major merger event, and only the most massive galaxies, which host the most massive BHs, are gas poor in the local Universe (Fanidakis et al. 2011, 2012).

A spin cut is in line with the longstanding speculation that these most relativistic jets require high spin BHs (Maraschi et al. 2012), and also gives a good match to the observed redshift distribution of BL Lacs which peaks at $z = 0.5$ and then drops off sharply, with no objects above $z \sim 2$. This is a consequence of three factors.

(i) BL Lac jets are restricted to BHs with $\dot{m} < 10^{-2}$, and there are no BHs accreting at $\dot{m} < 10^{-2}$ above $z \sim 2$.
(ii) Only the most massive BHs have high spin through mergers, which happen at late times, causing the bulk of the population to fall below $z = 1$.
(iii) These most massive objects are rare in the local Universe causing the distribution to decrease again below $z = 0.5$.

Since FRI sources are consistent with being the misaligned analogues of BL Lacs, they should also have high spin. They are indeed offset from the Fundamental Plane, i.e. have higher (mass corrected) core radio emission to the lower mass and presumably lower spin LINERs, though only by a factor of ∼10 (Broderick & Fender 2011). However, the radio emission is not predominantly produced from the same region as the *Fermi* flux so may not be as sensitive to the difference in spin.

ACKNOWLEDGEMENTS

We thank Nikos Fanidakis and the Millennium Simulation for use of their data. This work has made use of Ned Wright's Cosmology Calculator (Wright 2006). EG acknowledges funding from the UK STFC.

REFERENCES

Best P. N., Heckman T. M., 2012, MNRAS, 421, 1569
Bîrzan L., Rafferty D. A., McNamara B. R., Wise M. W., Nulsen P. E. J., 2004, ApJ, 607, 800
Blandford R. D., Znajek R. L., 1977, MNRAS, 179, 433
Broderick J. W., Fender R. P., 2011, MNRAS, 417, 184
Chiaberge M., Celotti A., Capetti A., Ghisellini G., 2000, A&A, 358, 104
Czerny B., Hryniewicz K., 2012, J. Phys.: Conf. Ser., 372, 012013
Dermer C. D., Mernon M., 2009, High Energy Radiation from Black Holes: Gamma Rays, Cosmic Rays, and Neutrinos. Princeton Univ. Press, Princeton, NJ
Dermer C. D., Schlickeiser R., Mastichiadis A., 1992, A&A, 256, L27
Done C., Gierliński M., Kubota A., 2007, A&AR, 15, 1
Esin A. A., McClintock J. E., Narayan R., 1997, ApJ, 489, 865
Falcke H., Körding E., Markoff S., 2004, A&A, 414, 895
Fanidakis N., Baugh C. M., Benson A. J., Bower R. G., Cole S., Done C., Frenk C. S., 2011, MNRAS, 410, 53
Fanidakis N. et al., 2012, MNRAS, 419, 2797
Fender R. P., Belloni T. M., Gallo E., 2004, MNRAS, 355, 1105
Ghisellini G., Tavecchio F., 2008a, MNRAS, 386, L28
Ghisellini G., Tavecchio F., 2008b, MNRAS, 387, 1669
Ghisellini G., Tavecchio F., 2009, MNRAS, 397, 985
Ghisellini G., Maraschi L., Treves A., 1985, A&A, 146, 204
Ghisellini G., Tavecchio F., Foschini L., Ghirlanda G., Maraschi L., Celotti A., 2010, MNRAS, 402, 497 (G10)
Ghisellini G., Tavecchio F., Foschini L., Ghirlanda G., 2011, MNRAS, 414, 2674
Heinz S., 2004, MNRAS, 355, 835
Heinz S., Sunyaev R. A., 2003, MNRAS, 343, L59
King A. R., Pringle J. E., Hofmann J. A., 2008, MNRAS, 385, 1621
Kneiske T. M., Dole H., 2010, A&A, 515, A19
Krause M., Alexander P., Riley J., Hopton D., 2012, MNRAS, 427, 3196
Maraschi L., Colpi M., Ghisellini G., Perego A., Tavecchio F., 2012, J. Phys.: Conf. Ser., 355, 012016
Martínez-Sansigre A., Rawlings S., 2011, MNRAS, 414, 1937
Merloni A., Heinz S., di Matteo T., 2003, MNRAS, 345, 1057
Murray N., Chiang J., 1997, ApJ, 474, 91
Narayan R., McClintock J. E., 2012, MNRAS, 419, L69
Narayan R., Yi I., 1995, ApJ, 452, 710
Nolan P. L. et al., 2012, ApJS, 199, 31
Padovani P., Urry C. M., 1990, ApJ, 356, 75
Padovani P., Urry C. M., 1991, ApJ, 368, 373
Padovani P., Urry C. M., 1992, ApJ, 387, 449
Russell D. M., Gallo E., Fender R. P., 2013, MNRAS, 431, 405
Satyapal S., Dudik R. P., O'Halloran B., Gliozzi M., 2005, ApJ, 633, 86
Shakura N. I., Sunyaev R. A., 1973, A&A, 24, 337
Shaw M. S. et al., 2013, ApJ, 764, 135
Sikora M., Begelman M. C., 2013, ApJ, 764, L24
Sikora M., Begelman M. C., Rees M. J., 1994, ApJ, 421, 153
Sikora M., Stawarz Ł., Lasota J.-P., 2007, ApJ, 658, 815
Springel V. et al., 2005, Nature, 435, 629
Tavecchio F., Ghisellini G., Ghirlanda G., Foschini L., Maraschi L., 2010, MNRAS, 401, 1570
Urry C. M., Padovani P., 1995, PASP, 107, 803
Urry C. M., Padovani P., Stickel M., 1991, ApJ, 382, 501
Volonteri M., 2012, Science, 337, 544
Volonteri M., Madau P., Quataert E., Rees M. J., 2005, ApJ, 620, 69
Volonteri M., Sikora M., Lasota J.-P., 2007, ApJ, 667, 704
Woo J.-H., Urry C. M., 2002, ApJ, 579, 530
Wright E. L., 2006, PASP, 118, 1711

APPENDIX A

The emission comes from a single zone of radius R. We assume material in the jet moves at a constant bulk Lorentz factor (Γ) and that some fraction of the transported electrons are accelerated into a power-law distribution between minimum and maximum Lorentz factors $\gamma_{\rm min}$ and $\gamma_{\rm max}$, of the form

$$Q(\gamma) = Q_0 \left(\frac{\gamma}{\gamma_{\rm b}}\right)^{-n_1} (1+\gamma/\gamma_{\rm b})^{n1-n2} = Q_0 q(\gamma) \qquad \text{for } \gamma_{\rm min} < \gamma < \gamma_{\rm max}, \quad \text{(A1)}$$

where $\gamma_{\rm b}$ is the Lorentz factor at which the electron distribution changes in slope from n_1 to n_2. We calculate the normalization Q_0 from the power injected into the accelerated electrons ($P_{\rm rel}$):

$$P_{\rm rel} = \frac{4\pi}{3} R^3 m_{\rm e} c^2 Q_0 \int_{\gamma_{\rm min,inj}}^{\gamma_{\rm max}} \gamma q(\gamma)\, {\rm d}\gamma. \quad \text{(A2)}$$

We calculate $\gamma_{\rm cool}$ after a light crossing time $t_{\rm cross} = R/c = \gamma_{\rm cool}/\dot{\gamma}_{\rm cool}$, as

$$\gamma_{\rm cool} = \frac{3 m_{\rm e} c^2}{4\sigma_{\rm T} R U_{\rm seed}}, \quad \text{(A3)}$$

where $U_{\rm seed} = U_B + U_{\rm sync}$ is the sum of the energy density in magnetic fields and synchrotron emission which provides the seed photons for cooling.

We solve the continuity equation to find the self-consistent steady state electron distribution:

$$N(\gamma, t_{\rm cross}) = Kn(\gamma) = \begin{cases} A Q_0 q(\gamma) & \text{for } \gamma_{\rm min} < \gamma < \gamma_{\rm cool}, \\ \frac{3 m_{\rm e} c^2}{4\sigma_{\rm T} c U_{\rm seed}} \frac{Q_0}{\gamma^2} \int_{\gamma}^{\gamma_{\rm max}} q(\gamma)\, {\rm d}\gamma & \text{for } \gamma_{\rm cool} < \gamma < \gamma_{\rm max}, \end{cases} \quad \text{(A4)}$$

where A is found by matching at $\gamma_{\rm cool}$.

We use the delta function approximation and calculate the synchrotron emissivity as

$$j_{\rm sync}(\nu) = \frac{\sigma_{\rm T} c}{6\pi\nu_B} U_B \gamma N(\gamma), \quad \text{(A5)}$$

where the electron Lorentz factor and synchrotron photon frequency are related by $\gamma = \sqrt{3\nu/4\nu_B}$ and we calculate the synchrotron self-absorption frequency ($\nu_{\rm ssa}$) as given by (Ghisellini, Maraschi & Treves 1985)

$$\nu_{\rm ssa} = \left(4.62 \times 10^{14} K B^{2.5} \frac{R_{\rm j}}{0.7}\right)^{2/7}. \quad \text{(A6)}$$

We calculate SSC emission including the Klein–Nishina cross-section using the delta approximation:

$$j_{\rm comp}(\nu) = \frac{\sigma_{\rm T} c}{6\pi} \int_{\gamma_{\rm min}}^{\gamma_{\rm max}} \int_{\nu_{\rm ssa}}^{\nu_{\rm sync,max}} \frac{U_{\rm sync}(\nu_{\rm sync})}{\nu_{\rm sync}} \gamma N(\gamma)\, {\rm d}\nu_{\rm sync}\, {\rm d}\gamma, \tag{A7}$$

where electron Lorentz factor and Compton photon frequency are related by $\gamma = \sqrt{3\nu/4\nu_{\rm sync}}$.

Bulk motion of the jet boosts and blueshifts the emission. We calculate the observed flux as

$$F(\nu\delta/(1+z)) = \frac{(j_{\rm sync}(\nu) + j_{\rm comp}(\nu))}{R_{\rm co}^2} \frac{4\pi}{3} R^3 \delta^3, \tag{A8}$$

where $\delta = (\Gamma - \cos\theta\sqrt{\Gamma^2 - 1})^{-1}$ is the Doppler factor, and $R_{\rm co}$ is the comoving distance to the object at redshift z.

This paper has been typeset from a TEX/LATEX file prepared by the author.